Monomer diffusion and polymer alignment in domains of sickle hemoglobin

Michael R. Cho and Frank A. Ferrone
Department of Physics and Atmospheric Science, Drexel University, Philadelphia, Pennsylvania 19104 USA

ABSTRACT We have used polarized absorbance to observe the process of monomer accretion and polymer alignment which occurs in domains of sickle hemoglobin that are formed and maintained by laser photolysis. These diffusion and alignment processes have been studied as a function of initial concentration and temperature (initial and final), as well as beam size and domain number. Monomers are found to diffuse into growing polymer domains with a rate that is essentially temperature and concentration independent, but which depends on the size of the final domain boundaries, and the number of domains within a boundary. The final concentrations achieved are very close to those found in packed centrifugation experiments (50–55 g/dl) and are approximately independent of starting temperature and concentration. The influx of monomers is accompanied by polymer alignment, and the amount aligned is proportional to the amount diffused throughout the process. We propose that polymer alignment controls the influx of added monomers into the growing domain.

INTRODUCTION

Deoxygenated sickle hemoglobin (HbS) forms 14 stranded polymers by a process of nucleation from bulk solution (homogeneous nucleation) and by nucleation onto polymers already present (heterogeneous nucleation) (Ferrone Hofrichter and Eaton, 1985a, 1985b; Ferrone et al., 1980). A polymer array, or domain, is created by each homogeneous nucleation event. The heterogeneous nucleation process, originally postulated on the basis of extensive physico-chemical data, has now been confirmed by direct observation. (Samuel, Salmon, and Briehl, 1990).

At long times the domain assumes a spherical symmetry, (White and Heagan 1970) and the radial alignment of polymers, when viewed in thin slices between crossed polarizers, is visible as a Maltese cross (Basak, Ferrone, and Wang, 1988; Hofrichter, 1986; Mickols et al., 1985). Whereas a mechanism has been proposed for this alignment process, it cannot be regarded as established. (Basak, Ferrone, and Wang, 1988).

Because the monomers are far more mobile than the polymers they form, the immobilization of monomers in polymers permits an influx of additional monomers into the growing domain. Such an influx has been predicted theoretically, (Zhou and Ferrone, 1990) and observed experimentally (Cho and Ferrone, 1990). This process has been loosely termed diffusion, through other processes may also be operative and may actually be rate limiting.

In preliminary studies (Cho and Ferrone, 1990), the time dependence of monomer increase, and the weak temperature dependence of the characteristic times, supported the idea that the influx of monomer simply occurred by monomer diffusion after rapid polymer formation. However, the values for the diffusion constant were over an order of magnitude smaller than expected. Kam and Hofrichter (Kam and Hofrichter, 1986) used inelastic light scattering to probe diffusion and found the monomers inside well formed gels to possess the same local mobility as they had before gelation. Calculations using a radial growth model suggested that diffusion was rapid enough to insure constant monomer concentration during polymer formation (Zhou and Ferrone, 1990). Whereas the diffusion rate might well diminish as polymers form and crowd the domain, the initial behavior is unlikely to be dominated by such effects. A primary motivation for this study was therefore the further investigation of factors that might limit the monomer influx. Moreover, because the newly arrived monomers can themselves add to existing polymers or form new ones, the process of domain growth must be limited by some other means than simple monomer depletion, and the study of monomer transport might also give clues to such a mechanism.

Three lines of experimentation are employed in this paper. First, the experiments of Cho and Ferrone (1990) at the domain centers were extended by observing the effect of domain sizes, initial concentration, and number of domains on the rate and extent of monomer influx. Second, larger spatial regions were examined to compare alignment with total concentration increase at long times, and as a function of time. Finally, the effect of temperature at domain formation was examined by slowly varying the temperature after a domain had been formed.

In the simplest scheme for gelation, polymerization is followed by either diffusion or alignment, but each process can be regarded as complete so as to simplify discussion of the remaining events. In the work described in this report, alignment and diffusion have been observed

Michael Cho's present address is Department of Biological Chemistry and Molecular Pharmacology, Harvard Medical School, Boston, MA 02115.

Correspondence should be addressed to Frank Ferrone.

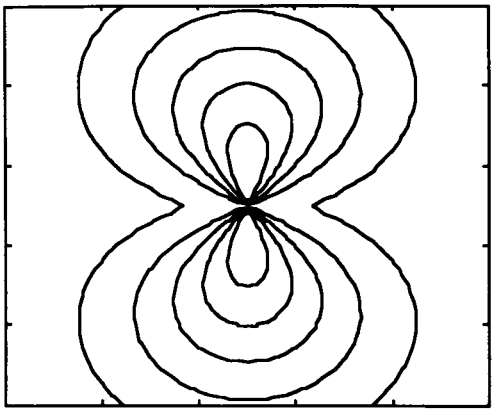

FIGURE 1 Theoretical contour map for the spatial variation of absorbance due to a radial array of anisotropically absorbing sickle hemoglobin polymers, viewed in linearly polarized light, oriented horizontally. The domain is centered in the frame. The concentration of the monomers in polymers falls off as a Gaussian towards the edges of the frame.

and are found to be intimately linked. Likewise, diffusion appears to be tightly coupled to polymer formation, so that an understanding of gelation must simultaneously encompass these three coupled processes.

METHODS

The apparatus and methodology have been described previously (Cho and Ferrone, 1990) and will only be summarized here. Microscopic photolysis with a focused steady-state laser creates a region of deoxygenated hemoglobin in a small (4–6 μm thick) carboxyhemoglobin sample. A part of that region is observed by light scattering, birefringence intensity, or absorption. A two-dimensional image of any of these variables is collected; such a frame measures 50 × 50 μm. This frame is broken down into 1-μm square data elements. Scattering of the 514-nm photolysis beam is used to identify the domain center and trigger data collection. The primary data collected in this experiment is polarized absorbance at 430 nm, which is near the peak of the deoxyhemoglobin absorbance spectrum. Absorbance and scattering frames are typically interleaved in a kinetic experiment. For confirmation of the number of domains, the polarizers, which are located before and after the sample, are crossed and the sample is observed at 488 nm. A single domain is characterized by a well resolved "Maltese cross" pattern.

Because hemoglobin polymers are not optically isotropic absorbers, conversion of absorbance to hemoglobin concentration requires knowledge of polymer alignment. If the extinction coefficient of hemoglobin isotropically averaged in solution is ϵ_0, the coefficient for light polarized parallel or perpendicular to the fibers is $0.34\epsilon_0$ and $1.33\epsilon_0$, respectively. (Eaton and Hofrichter, 1981). A collection of fibers which lies randomly distributed in the plane of the sample would thus have an extinction coefficient of $0.84\epsilon_0$. This will create problems of interpretation as we will discuss later. Sickle hemoglobin polymer domains assume radial symmetry, with polymer density falling off roughly as a Gaussian (Basak, Ferrone, and Wang, 1988), and such a radial pattern of polymers gives a distinctive appearance when viewed in polarized light such as that shown in Fig. 1. In this figure, contours at different absorbances have been plotted over an area equal to the one scanned in these experiments. As can be seen, though the polymer density is radially symmetric, the absorbance shows a figure eight or "pinched" contour, whose major axis follows that of the polarizers.

Sample temperature was regulated by a Cambion thermoelectric stage and a computer interfaced controller of our own design. The laser spot size was measured by scattering from a layer of latex particles. The scattered intensity was fit to a skewed Gaussian as described. To decrease the size of the photolysis spot for some experiments, a beam expander was constructed from two simple lenses and an iris. This reduced the beam size from ~24 μm radius to ~10 μm.

RESULTS

Monomer transport was monitored by collecting typically 13 frames of polarized absorption as a function of time. Fig. 2 shows a sampling of the contours of absorbance accompanying the increase in concentration for a 33.5 g/dl sample in which many domains have formed. The argon laser initially converts the CO-hemoglobin to deoxygenated hemoglobin in the region shown by the

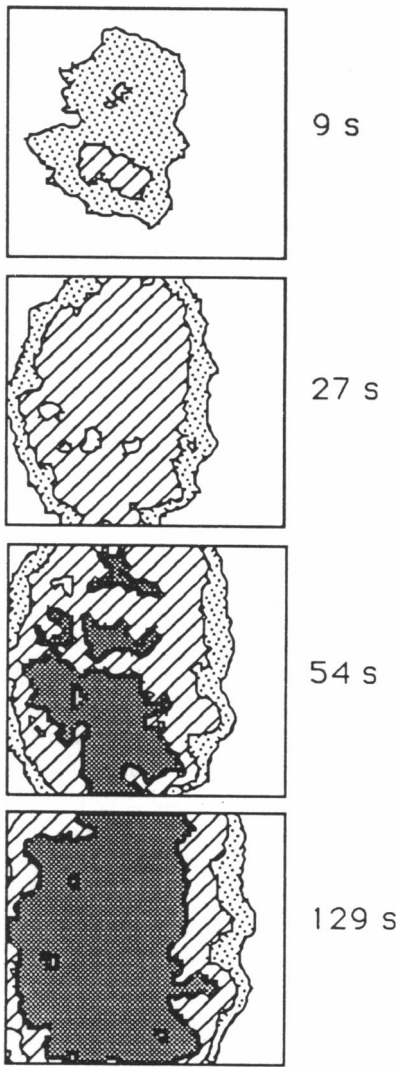

FIGURE 2 Experimental absorbance contours viewed in polarized light for a multidomain sample. The window is a 50-μm square. The contours are drawn at 0.1-OD increments, beginning with 0.5. The time at which each frame was collected is shown next to the frames. Sample concentration was 35.3 g/dl, at a temperature of 28.8°C. There is a small widening of the outer contour initially as the result of CO diffusion out of the illuminated area.

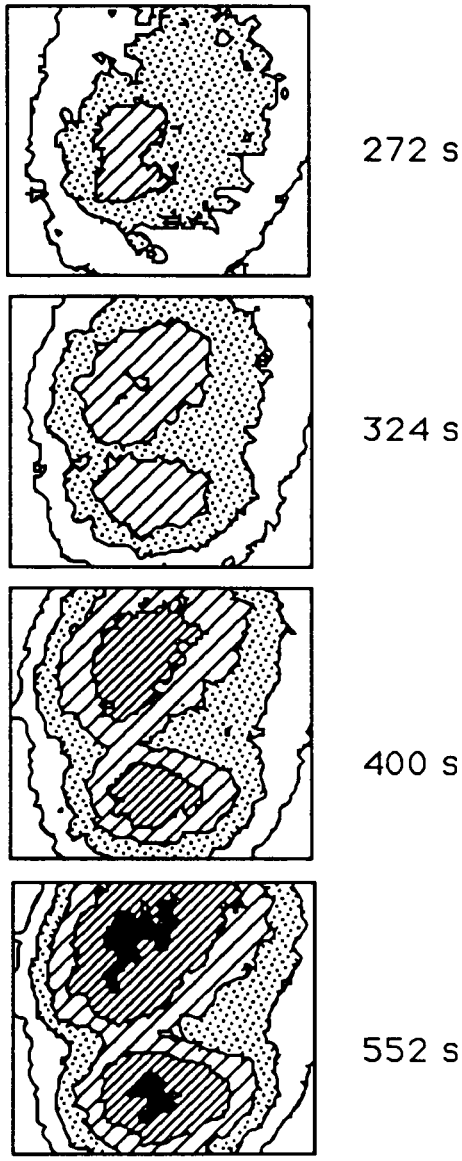

FIGURE 3 Experimental absorbance contours viewed in polarized light for a single domain sample. The window is again 50 μm square. The contours are drawn at 0.1-OD increments, beginning with 0.4. The time at which each frame was collected after initiation of photolysis is shown next to the frames. Note that the contours develop a "pinched" appearance, similar to the theoretically expected contours of Fig. 1. When viewed between crossed polarizers, a well defined "Maltese cross" was seen centered about the narrow point in these pinched contours. Sample concentration was 33.5 g/dl, at a temperature of 19.6°C. The size and shape of the outer contour is set by the laser beam.

outer contour, which remains essentially fixed throughout the experiment, being set by the laser beam size and oval shape. (There is a small widening of the outer contour initially as the result of CO diffusion out of the illuminated area). As polymers form, the total absorbance increases due to the influx of additional monomers.

In contrast, Fig. 3 shows an experiment in which a single domain had formed, as subsequently verified by observing the light transmitted when the sample is placed between crossed polarizers. Due to the anisotropic absorbance of aligned polymers, the contours do not retain the oval shape of the laser beam, but develop a pronounced "pinch" in the center. As shown in Fig. 1, this is expected from an array of radially aligned polymers. When the polarizers are both rotated the pattern rotates in similar fashion.

Kinetics at the domain center

We have previously reported initial results in which the center of the domain was analyzed (Cho and Ferrone, 1990), where the lack of birefringence allowed the assumption that polymers were either totally randomly aligned (i.e., in all three directions) or planar-random (i.e., distributed in random orientations in the plane of the sample). The concentration of excess hemoglobin, defined as that above the initial concentration, irrespective of polymerization state, was found to increase with a long tail similar to that seen in diffusive processes. The data was fit well by a simple diffusion model in which the concentration of diffused hemoglobin c_+ is given by

$$c_+ = c_+(\infty)\exp(-\tau/t), \qquad (1)$$

where $c_+(\infty)$ is the maximum amount of diffused material, and τ is the time constant.

Those experiments were extended here in three ways. First, a simple pair of lenses were used to decrease the laser beam size, to observe the effect of domain sizes on single domains at the same temperature and concentration. Second, initial concentration was varied. Third, multiple domains were investigated. In all cases the kinetic curves were similar as shown in Fig. 4, and were parametrized by Eq. 1 to obtain a time constant τ, and a final concentration. These results are summarized in Table 1.

There is essentially no effect of temperature (as shown previously) or concentration on the characteristic time τ. Reduction of the beam size from 23.4 to 10.5 μm constrains the maximum domain size and results in a significant decrease in τ (almost a factor of 3) with almost no change in final concentration, $c_+(\infty)$. The presence of multiple domains also leads to a decrease in the characteristic time. Although the concentration in the multidomain experiment is higher than that for the single domain experiments, we did not expect this to have an effect per se, inasmuch as no concentration dependence was seen for single domains. In contrast to the behavior of single domains, the multidomain experiment shows a distinct temperature dependence.

Spatially extended observations

The preceeding data is obtained from analysis at the center of the domain. By examining larger spatial regions, alignment could also be observed. Aligned polymers absorb differently in different directions: this is the physical origin of the pinched contours in Fig. 3. The

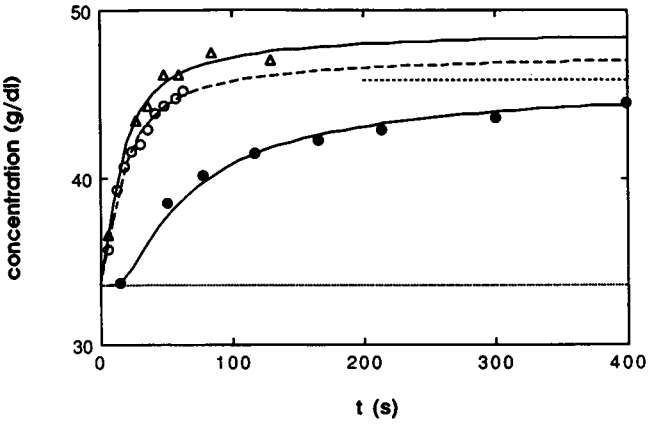

FIGURE 4 Increase in concentration at the domain center as a function of time. Zero time is set by the initiation of light scattering, which signifies domain formation. There is a delay between laser-induced desaturation of the sample and domain formation. When a single domain is formed, the delay exhibits stochastic fluctuations. Characteristic times are shortened by either reducing beam size or producing multiple domains. The lines through the data are the results of least squares fitting of the excess concentration by Eq. 1. Filled circles show a single domain, with a laser beam of 23.4 μm radius. Initial concentration was 33.5 g/dl (shown by the *horizontal line*), temperature was 18.1. The extrapolated final concentration is shown as the short dotted line, and is 45.8 g/dl. Characteristic time τ was 102 s. Triangles show a single domain created with a reduced beam size of 10.5 μm, and initial concentration again 33.5 g/dl, and a temperature of 29°C. Asymptotic concentration was 48.8 g/dl, and the characteristic time was shortened to 11.5 s. Open circles describe a multidomain sample (analyzed at the beam center). The laser beam was 23.4 μm, initial concentration was 35.3 g/dl, and the temperature was 19.2°C. The asymptotic concentration here is 50.2 g/dl, and the characteristic time is 15.1 s.

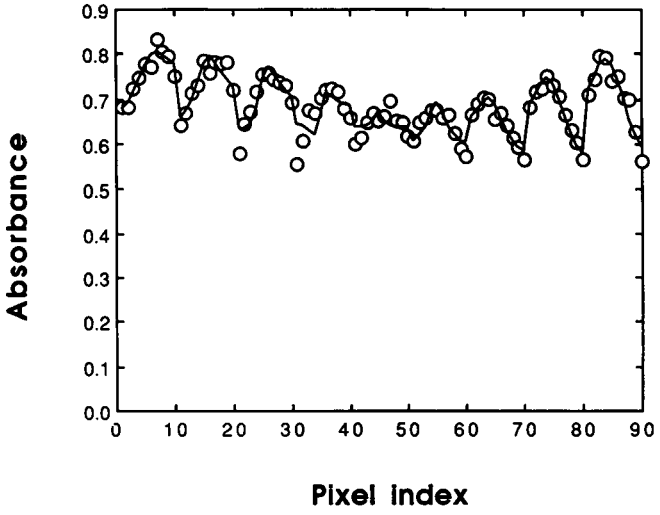

FIGURE 5 Absorbance of a 10 × 10-μm region in the center of a frame of data. Data elements were 1 μm square. One row is eliminated (giving 90 data elements total), so that the domain center can line on a row. The experiment is part of a temperature cycling experiment. The initial concentration was 33.5 g/dl; the sample temperature was 25.0°C. Data has been fit by Eq. 2. Note that the oscillatory behavior, which arises from alignment, sits on a large pedestal. Part of the pedestal is due to absorption by aligned polymers in the weak direction, but the greater part is from absorption of randomly oriented polymers and monomers.

concentration of aligned polymers can be determined by the measurement of linear dichroism, the difference in absorption in two perpendicular directions. Linear dichroism could be equally measured by rotating the polarizers by 90°, or by rotating the sample of polymers 90°. If the polymers are aligned radially, then another method is to compare the absorbance of polymers oriented vertically in one part of the domain with absorbance of polymers oriented horizontally in a different part of the domain, rather than rotate the polymers at one specific part of the domain. This does involve the assumption of radial alignment, and the validity of this particular assumption will be discussed below. It has the major advantage that it is readily used in kinetic experiments, however.

TABLE 1 **Kinetic data**

c_o	T	Beam R	Number of domains	Final c*	τ*
g/dl	°C	*μm*		*g/dl*	*s*
33.5	17.2	23.4	1	45.1	64
31.3	17.2	23.4	1	42.7	69
28.9	17.2	23.4	1	43.9	40
33.5	29.0	10.5	1	48.1	12
35.2	19.5	23.4	>1	50.1	12
35.2	28.8	23.4	>1	49.6	6

* Obtained by fitting to Eq. 1.

To analyze the amplitude information it is helpful to represent that data as a series of data points (x-axis) versus the absorbance, rather than a two dimensional array. In doing this, elements of the second row are listed after the first row and so on. Thus, the rows, or tracks, are plotted in sequence as shown in Fig. 5. A 10 × 10-μm area, consisting of 10 tracks of 10 points each, is shown, which was centered on the domain. The absorbance differs at each point because the point corresponds to a different angle between polymer axis and polarizer axis.

To account for a small spatial drift of the domain center, presumably due to small motions of the coverslips that contained the sample, the center of analysis was consistently taken as the center of the pinched contours. This also prohibited the use of data much beyond a 10 × 10-μm square.

Within each track the absorbance peaks when the polymer axis lies perpendicular to the polarizer axis. This gives the picture an oscillatory appearance. Each period of this oscillation corresponds to one of the ten "tracks". Even with perfect alignment, the minimum absorbance is not zero, because the polymers absorb even in the weak direction. The anisotropic absorbance is readily converted to aligned polymer concentration. Absor-

bance is converted to intensity, which is then fit by least squares to the theoretical angular dependence.

Each pixel coordinate can be assigned an angle θ determined as the angle that a line between the pixel under study and the domain center makes with the polarizer axis. If the observed absorbance at a given pixel is A, then let $E = 10^{-A/2}$ and the data should show behavior

$$E = E_1 \sin^2 \theta + E_2, \tag{2}$$

which can be easily derived from the anisotropic absorbing nature of the polymers. (Cho, 1990). We define decay coefficients α which are related to extinction coefficients by

$$\alpha = (2.303/2)\epsilon lc. \tag{3}$$

If α_s and α_p are decay coefficient perpendicular and parallel to the polarizer axis, then

$$E_1 = \exp(-\alpha_p) - \exp(-\alpha_s) \tag{4a}$$

$$E_2 = \exp(-\alpha_s), \tag{4b}$$

in which

$$\alpha_s = \alpha_0 + 1.34\alpha_A \tag{5a}$$

$$\alpha_p = \alpha_0 + 0.34\alpha_A. \tag{5b}$$

Here α_A is the aligned (isotropic) hemoglobin decay coefficient, composed from the isotropic extinction coefficient and the aligned hemoglobin concentration. α_0 is the average coefficient from monomers and unaligned polymers in the solution. The expected minimum absorbance is clearly the result of the isotropic contribution (α_0) and the aligned contribution (α_A).

Examination of the magnitude of the absorbance shows that the oscillatory part sits on a pedestal larger than simply accounted for by the smallest absorbance of aligned polymers, i.e., that $\alpha_0 \neq 0$. This α_0 consists of absorbance due to monomers, and absorbance from polymers with no net alignment. The polymer orientation may either be truly random or planar random. The two types of random polymers will have different extinction coefficients. We assume that the appropriate extinction coefficient is that for three-dimensional isotropic absorbers, thereby implicitly assuming all isotropic polymer absorption comes from polymers which are truly random in three dimensions.

It was thus possible to determine the aligned and total concentrations for a given frame. Moreover, this could be done as a function of time. Both aligned and total concentrations were assumed constant across the small 10-μm window. This assumption is also discussed below. Thus, each frame was reduced to a single aligned concentration and a single isotropic concentration (and thus a single total for the frame).

The increase in aligned polymers occurred in parallel with the increase in total concentration. To examine the extent of this similarity, the ratio of aligned concentration to excess concentration is plotted in Fig. 6 as a function of time. Data are shown for three concentrations and two different temperatures. As can be seen, within the scatter of the data, the ratio quickly assumes a constant value. The line in the figure is the average ratio taken from a series of measurements made at much longer times (as described below). The kinetic data are clearly close to the line for a substantial part of the kinetic process. (One data set not shown had a higher overall and final value.)

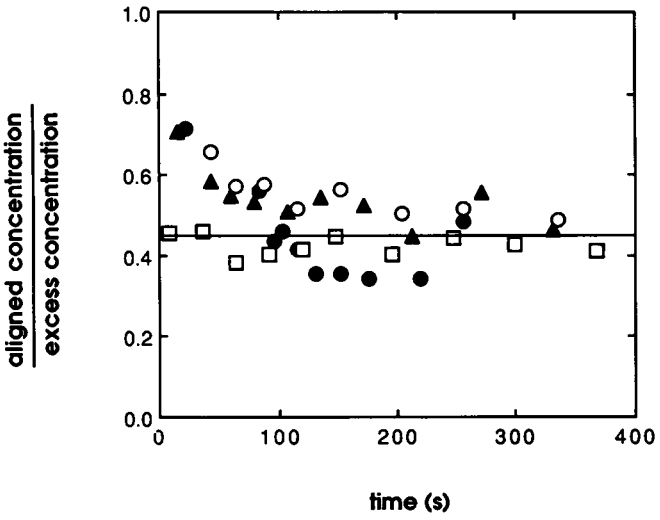

FIGURE 6 The ratio of aligned concentration to excess total concentration is shown as a function of time. By excess is meant the concentration above the initial concentration. Each concentration represents an average over the entire frame. Initial concentration for the filled symbols was 33.5 g/dl; for the open circles, 31.3 g/dl; and for the open squares, 28.9 g/dl. The horizontal line drawn is the average ratio obtained in the analysis of long time temperature variation. In terms of the text variables (cf. Eq. 6), the line is determined from c_{A0}/c_{T0}.

Temperature variation of preformed domains

Finally, we sought to examine what effect the formation temperature had on the gel. The temperature of a domain was slowly varied once it had been formed in order to determine the response of a preformed gel, and thereby separate the formation kinetics. The domain at each temperature was characterized by the average concentration taken over our smaller (10×10 μm) frame as described above. Samples of 33.5 g/dl initial concentration were polymerized at 22.5, 16.5, 13.0, and 9.8°C. Temperatures were changed at a rate of 0.17°C/min after polymerization. Experiments typically lasted 4 to 5 h, with data collected roughly every half hour. Temperatures were explored above and below the temperature at which the domain was formed. In no cases did the temperatures form a monotonic sequence; after reaching a maximum or minimum, the range was retraced.

TABLE 2 **Effect of temperature on preformed gels**

		Three parameter fit (Eq. 6)				Two parameter fit (Eq. 6)		
T_0*	T range‡	a_T	b_T	c_{T_0}	χ^2	b_T	c_{T_0}	χ^2
		g/dl/°C	*g/dl/h*	*g/dl*		*g/dl/h*	*g/dl*	
16.5	16.5–25.1	0.23 ± 0.28	1.36 ± 0.84	43.5 ± 5.4	1.04	1.62 ± 0.78	47.9 ± 1.0	0.69
22.5	12.5–22.5	0.13 ± 0.20	0.60 ± 0.58	44.1 ± 3.9	0.04	0.44 ± 0.54	47.0 ± 0.9	0.10
13.0	11.1–30.8	0.01 ± 0.04	1.54 ± 0.20	48.1 ± 1.0	0.99	1.54 ± 0.20	48.3 ± 0.4	0.75
9.8	9.8–30.9	−0.03 ± 0.19	1.76 ± 1.16	48.7 ± 2.1	0.31	1.58 ± 0.42	48.4 ± 0.7	0.21

* Temperature at which the sample was polymerized. ‡The range was not traversed in one direction.

From the kinetic experiments above we originally judged the rate of temperature change to be slow enough to maintain equilibrium. However, when the data was analyzed subsequently, there was evidence for a small drift, e.g., when a given temperature was reset, the final concentration was slightly higher. To account for the drift, and to assess the dependence on temperature, the total concentration c_T averaged over each frame was fit to a linear function of time (t) and temperature (T), i.e.,

$$c_T = c_{T0} + a_T T + b_T t. \quad (6)$$

The subscript T indicates total concentration.

Excellent fits were obtained ($\chi^2 < 1$), however, the temperature coefficients a_T were all consistent with zero, implying no temperature dependence. Consequently, the data were fit to a simpler linear function of time (i.e., set $a_T = 0$), again obtaining excellent fits. Four replicate experiments showed highly consistent results of 48 g/dl as the concentration c_{T_0} (Table 2). Because the drift is only modelled in a linear fashion, the number quoted for c_{T_0} is that obtained at the start of temperature cycling.

The aligned and unaligned parts (denoted by A and U) were separately analyzed in a similar fashion. The relative uncertainties in the average values of the drift coefficient b included zero drift in both unaligned and aligned cases. However, it was also evident that the drift of the total concentration was included in the range of drifts seen in the aligned and unaligned concentrations. Interestingly, the temperature dependence was nonzero, and of opposite sign: the unaligned concentrations increase with temperature ($a_U = 0.20 \pm 0.11$ g/dl/°C), whereas the aligned concentrations decrease with temperature ($a_A = -0.14 \pm 0.10$ g/dl/°C).

Since the concentrations obtained by the kinetic analysis are obtained from the domain centers, where there is no alignment, we thought they might be comparable with the unaligned concentrations obtained as the temperatures were cycled. Fig. 7 shows such a comparison. The open symbols are the cycled temperatures taken for four distinct runs without correction for drift; the filled symbols are obtained from the extrapolated fit described by Eq. 1. The agreement is quite good. It is also interesting that the best fit to all the data shows a slope only slightly higher than the values of b seen in the fits to two variables, indicating that displaying the data without drift correction makes little effect on the results.

Assumption of uniformity

Finally we turn to the assumptions of uniformity. To justify reducing the frames to a single concentration we need to show that the concentrations show no systematic deviation in space, and that the different parts of the domain have the same kinetic behavior.

To assess spatial uniformity we used the data taken at various temperatures to construct a composite picture. Each track in a frame can be fit by Eq. 2 to give an aligned, unaligned, and total concentration. Values for each given track where then averaged across all the tem-

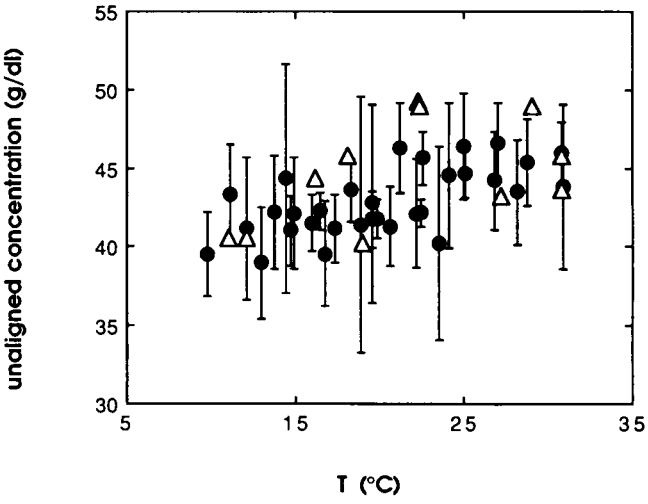

FIGURE 7 Comparison of unaligned concentration obtained by different methods. The frame averaged unaligned concentration (as determined by curvefitting to Eq. 2) is drawn as filled circles as a function of temperature for four experiments that began with the same concentration of 33.5 g/dl. Error bars represent the standard deviation of the average. The open triangles are the points determined by fitting kinetics observed at the center of the domain to Eq. 1. At the domain center there is no net alignment; hence, the total concentration is the unaligned concentration. (The open triangles are the same data as published by Cho and Ferrone [1991].)

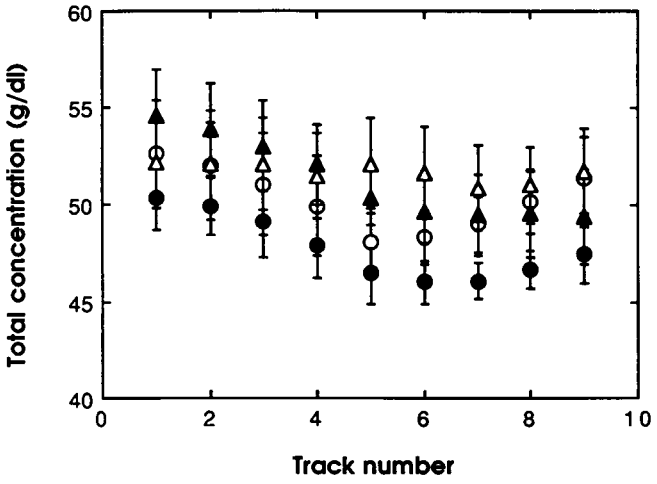

FIGURE 8 Averaged total concentrations for four experiments at 33.5 g/dl initiated at different temperatures. Each of the nine tracks in each experiment were fit by Eq. 2 to obtain the aligned and unaligned concentrations whose total is shown. The concentrations of each track were averaged across all experiments; the error bars show the deviations from the averages. Variation with track number is less than the sample-to-sample variation; the variation is primarily due to the aligned concentration (cf. Fig. 9).

peratures investigated, and the set of averages examined. The assumption was that any systematic track-to-track variation would become apparent. The total concentration showed a small dependence as seen in Fig. 8 for four experiments. Since the variation between experiments is greater than the variation within a given set of data, assuming a constant total concentration is a reasonable approximation. There is a small systematic dip towards the center, which arises from the aligned polymers. As shown in Fig. 9, the concentration of aligned polymer increases with distance away from the center of the domain. Since modeling the radial dependence would have entailed an additional parameter of unknown time and temperature dependence, it was decided to treat the aligned concentration as constant, with the caveat that there is greater variation than seen in the total concentrations. This is clearly an oversimplification. This was the only part of the analysis in which tracks from different frames are averaged together.

To justify the use of frame averaging for kinetic data, we examined the spatial dependence of the influx. Fig. 10 *a* shows kinetic curves at two different radii. As is evident, the time course and extent of reaction are virtually identical. Conversely, we also examined the radial dependence at different times. Fig. 10 *b* shows the radial dependence at three different times. It is clear that there is little or no concentration gradient in this region. The data in Fig. 10 describe a rather uniform concentration of polymers across the viewed area during the time of monomer influx, which supports the use of a single frame average to describe the kinetics.

DISCUSSION

Final concentrations

The maximum concentrations spontaneously achieved in these studies exceed 48 g/dl, and are quite similar to concentrations achieved by centrifugation which are in the range of 50–55 g/dl (Hofrichter, Ross, and Eaton, 1976; Sunshine, Hofrichter, and Eaton, 1979). Two factors suggest that the similarity is even greater, i.e., that our value represents a lower limit. First, the concentration has been averaged over the domain. The aligned polymers show a small but definite variation with distance from the center: at the edge the polymer concentration is ~10 g/dl, whereas in the central track the concentration is ~5 g/dl. The central region is lower, most likely, because the polymers in the isotropic part are planar random rather than three-dimensional random, and this leads to an underestimate of the extinction by ~14% of the polymers. For this reason, the maximum concentration may be ~2 g/dl higher.

Furthermore, in the experiments in which temperature was slowly cycled, the observed maximum concentrations showed a persistent but small drift. This occurred despite systematic attempts to account for effects such as small motions of the coverslips. It seems likely that the "drift" represents a physical, unavoidable process, such as the continued alignment of polymers at a very slow rate. This is supported by the fact that this drift

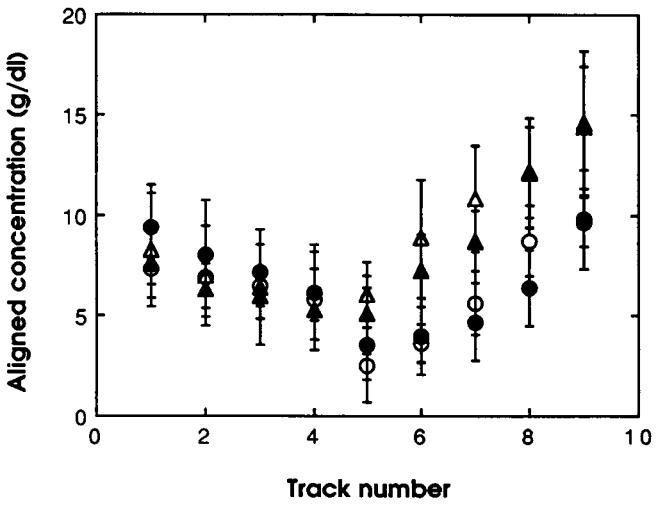

FIGURE 9 Averaged aligned concentrations for four experiments at 33.5 g/dl initiated at different temperatures. Each of the nine tracks in each experiment were fit by Eq. 2 to obtain the aligned concentrations. The concentrations of each track were averaged across all experiments; the error bars show the deviations from the averages. There is a small consistent variation across the different tracks (i.e., from top to bottom.) Representing the frame by a single aligned concentration thus represents an oversimplification whose magnitude may be appreciated by the size of the errors and deviations from a horizontal average in this figure.

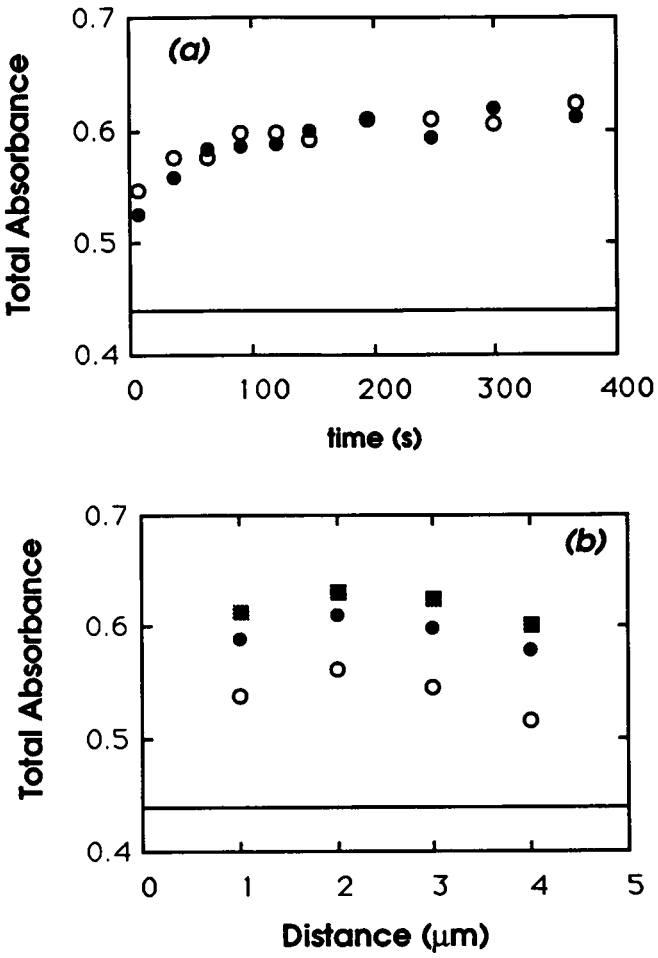

FIGURE 10 (*a*) Increase in absorbance (due to monomer influx) at distances of 1 μm (*open circles*) and 5 μm (*filled circles*). (*b*) Spatial absorbance profiles for the same experiments at three different times during polymerization. Data was taken on a sample of 28.9 g/dl initial concentration, and a temperature 18.5°C. The similarity of data at different radii, and of profiles at different times, suggests that a single concentration may adequately represent the kinetics of the monomer influx.

always increases the total concentration, whereas uncontrolled experimental variables would be more likely to produce effects of both signs. The separate analysis of aligned and unaligned concentrations ought to show alignment increasing, but because the error range of the separate analysis of the data (vide supra) encompassed zero drift, it was impossible to follow the individual contributions of aligned and unaligned polymers over long times. Such slow, continued alignment has been observed by others, albeit in multidomain samples (Ross, Hofrichter, and Eaton, 1974).

It is important to note that the correction of these temporal drifts described above were all done downward, to the initiation point. (Since the data was only sufficient to fit a linear function, we did not attempt to find an asymptotic value.) However, if we consider that a 5-h experiment with a 1.6 g/dl drift per hour would increase the final concentration by 8 g/dl, the 48 g/dl cited above rises to 56 g/dl. The similarity to the centrifugation results is quite interesting considering that the centrifugation experiments occurred over the course of hours, under pressures easily amounting to 100 atm.

Prouty, Schechter, and Parsegian (1985) performed a series of osmotic stress experiments in which osmotic pressure was used to alter the concentration of HbS in dialysis tubes. By comparison of non-gelling hemoglobin concentration at the same osmotic pressure, we can compare those results with our own. In the 20 to 30°C range, the results are similar to ours and those of Sunshine (close to 50 g/dl) but at lower temperatures, a distinct decrease was found in the osmotic measurements. Unfortunately, data were not taken from 20 to 3°C, at which temperature the final concentration for a 33.5 g/dl sample was only ~39 g/dl. We do not find such a decrease in the intermediate regime, though our data was not taken so low. (It is thus conceivable that some phenomenon causes the final concentration in our experiments and those of Prouty to drop abruptly when the temperature is below some critical temperature.) In the previous work, gels were necessarily multidomain structures. Our experiments investigated either single domains or domains that have a smaller surface to volume ratio, and thus are more representative of the interior features of domains. (With our typical beam size and sample thickness, we have eight times less surface area than the equivalent spherulite.) Thus, the comparison to the osmotic pressure experiments may well be limited. The experiments of Sunshine et al. (1979) are distinct from the osmotic experiments because pressures there are much greater than found in the osmotic experiments.

It is noteworthy that the aligned and unaligned polymer concentrations have opposite temperature dependences. The unaligned concentrations increase with temperature (0.20 ± 0.11 g/dl/°C), whereas the aligned concentrations decrease with temperature (-0.14 ± 0.10 g/dl/°C). The monomer phase is included in our definition of unaligned concentration. If the concentration of the monomer phase is proportional to the solubility, then the temperature dependence of the monomer phase implicitly includes the temperature dependence of the solubility. The solubility decreases with temperature, changing at a rate of −0.4 g/dl/°C over the range covered by these experiments. Unfortunately, it is not clear what fraction of the sample will be monomers and polymers so as to cleanly separate these contributions. If we adopt the approximation that the fraction is similar to that seen by Sunshine et al. (1979), then 35% of the unaligned hemes are in the monomer phase. Therefore the monomer contribution is −0.14 g/dl/°C, giving the unaligned polymer concentration a temperature coefficient of +0.34 g/dl/°C. Hence, as temperature increases, the total polymer concentration rises whereas the aligned polymer concentration decreases. The forces

driving alignment cannot therefore simply reflect those which drive polymerization. In particular, the sign of the temperature coefficient for the alignment process would argue against its being hydrophobically driven. Overall, the temperature dependence of the aligned and unaligned polymer concentration, and their opposing trends, suggests that factors other than simple packing constraints are operative in determining the final polymer density and state of alignment.

Kinetics

At present we have no entirely satisfactory explanation that unifies all our kinetic findings. These findings are: (*a*) that monomers diffuse into growing polymer domains with a rate that is essentially temperature and concentration independent, but which depends on the size of the final domain boundaries, and the number of domains within a boundary; (*b*) that the influx of monomers is accompanied by polymer alignment; (*c*) and that the amount aligned is proportional to the amount diffused throughout the process.

The first question in developing a mechanism is that of diffusion control. If the monomer influx is not limited by monomer diffusion, it may be limited by the rate of polymer growth. The growth of polymers, in turn, may be limited by the availability of free polymer ends. We shall discuss these points in turn.

A number of our observations are consistent with a simple, diffusion controlled process, such as the weak temperature and concentration dependence. Similarly expected is the decrease in characteristic time when the beam size is reduced. If the beam size is R, the characteristic time should vary as $1/R^2$, so that the characteristic time of 64 s is predicted to drop to 13 s, which is almost perfect agreement with the 12 s observed (Table 1). However, direct measurements reveal that the rate of polymer growth is significantly smaller than that of diffusion controlled reactions. The only way in which diffusion control could be exercised, therefore, is by postulating slow diffusion. Whereas a decrease in the diffusion constant might be expected near the completion of the reaction, a decrease in the early stages of domain growth is hard to understand. Moreover, describing the monomer influx as diffusion controlled provides no explanation for the experiment in which multiple domains are produced. In that experiment, despite the same beam geometry and a higher initial concentration, the rate of influx is significantly faster. It would be necessary to postulate that the diffusion-diminishing obstruction is less effective for the multidomain case than for single domains. And, because the final concentrations are the same, the effect must be purely kinetic.

Explanations other than diffusion control are only slightly more appealing. For example, the known value of diffusion coefficients (Hall, Oh, and Johnson, 1980; Kam and Hofrichter, 1986) suggests that diffusion ought to be much faster than polymer growth. If rapid diffusion is assumed, then the rate of monomer influx is limited either by the rate of growth of polymers or by the accessibility of polymer ends.

Suppose the added monomers simply reflect the total polymerized monomer population, so that the rate of influx observed is just the rate of monomer incorporation into polymers. This hypothesis would explain the constancy of the aligned fraction as arising from the presumed domain structure. In the multiple domain experiment, the higher concentration gives rise to faster polymer growth and hence should speed up the influx of monomers to compensate for those consumed in growth. On the other hand, this hypothesis requires single domains to also show faster monomer influx at higher concentrations, which they do not. But most perplexing would be the experiment in which the beam size was reduced. In that case, events at the domain periphery would directly affect the polymer growth rate at the center.

In experiments such as these, a virtually infinite reservoir of monomers is available, so that the reaction must cease due to crowding, rather than monomer depletion. There are two aspects to crowding: inhibition of growth, and suppression of nucleation. Microscopically, crowding can inhibit further growth by the obstruction of polymer ends. This leads to a third hypothesis, namely that end obstruction is the controlling variable. Despite a number of difficulties, this hypothesis appears to be the one most consistent with our observations. The monomer influx is seen in this hypothesis as the result of the increased polymer alignment. Since aligned polymers have more free ends, the alignment of polymers promotes their growth, which in turn allows further monomer influx. This might also provide a common link between the reduced beam experiment and the multidomain experiment. In each case, the maximum polymer length is decreased. In fact, as the temperature is increased, the length ought to have further decreased, with a corresponding decrease in characteristic time, in agreement with observation.

Nonetheless, visualization of such a mechanism is not easy. For example, it is difficult to see that alignment controls the monomer influx, since direct observations (Samuel, Salmon, and Briehl, 1990) have revealed a cross-linked gel, making direct large scale fiber movement difficult to rationalize. On the other hand, the ends of growing polymers are seen to execute a type of Brownian fluctuation, so that it is conceivable that a polymer could "search out" a path for growth despite a region of obstruction. Then the rate of growth is effectively limited by the diffusional motion of the polymer end. Other mechanisms such as one that we have previously proposed, in which random length fluctuations at equilibrium lengthen the polymer size (Basak, Ferrone, and Wang, 1988), are hard to justify in alignment which occurs clearly before equilibrium is reached.

The number of obstructions may not be large. For fibers of micron length (Briehl, Mann, and Josephs, 1990), the number of ends to be obstructed are less than 1% of the number of polymerized monomers. Optical microscopy reveals polymer lengths of tens of microns, requiring only 0.1% of the monomers to be obstructed (Samuel, Salmon, and Briehl, 1990). Obstruction thus may be relatively rare and may be difficult to spot in other than a kinetic fashion. Since the heterogeneous nucleation process creates new polymers on the surface of existing ones, there is a predisposition for new polymers to track old ones. Hence, obstructions (other polymers) for the older members can obstruct new polymers as well. Likewise, polymers that grow to the domain periphery will cease active growth.

Finally, we turn to the question of continued heterogeneous nucleation. While the obstruction of polymer ends inhibits growth, what precludes further heterogeneous nucleation? Two things are to be noted. First, the surface areas available for nucleation will decrease as larger bundles of nucleated fibers are formed. This means that the nucleation rate will decrease. Second, the number of monomers available to a new nucleus could be small enough to further pose a kinetic barrier to nucleation. A nucleus is intrinsically unstable, and in the early stages of polymer formation, once a nucleus is formed it rapidly elongates. But monomers are also more stable than the nucleus, or species similar in size. In fact, if the nucleation barrier is symmetric, monomers are the most stable species until the polymer length is at least twice the size of the nucleus. If the growth rate is slow enough at this early stage, say due to the need to diffuse monomers into a local region, there remains a good chance for small polymers to "find" the monomer state and thereby disappear as they walk along the reaction path. This makes the net rate of new polymer formation even smaller.

The above mechanism clearly has a number of details to be worked out, and represents a number of conceptual difficulties. If correct, it suggests a radically new approach to understanding the gelation process. Previous gelation models employed a hierarchy of nucleation, growth, and alignment. With the double nucleation mechanism came the first suggestion that growth and alignment might occur simultaneously. The proposal presented above suggests that fairly early in the process of domain growth, alignment becomes rate limiting for continued polymer growth. This makes it imperative to understand these processes, for it is clear that processes such as obstruction and alignment can be operative, and in some cases may even be the decisive elements in the macroscopically early phase of gel formation.

Received for publication 4 October 1991 and in final form 13 March 1992.

REFERENCES

Basak, S., F. A. Ferrone, and J. T. Wang. 1988. Kinetics of domain formation by sickle hemoglobin polymers. *Biophys. J.* 54:829–843.

Briehl, R. W., Mann, E. S., and R. Josephs. 1990. Length distributions of hemoglobin S fibers. *J. Mol. Biol.* 211:693–698.

Cho, M. R. 1990. Monomer diffusion and polymer alignment in domains of sickle hemoglobin. Ph.D. Thesis, Drexel University, Philadelphia.

Cho, M. R., and F. A. Ferrone. 1990. Monomer diffusion into polymer domains in sickle hemoglobin. *Biophys. J.* 58:1067–1073.

Eaton, W. A., and J. Hofrichter. 1981. Polarized absorption and linear dichroism spectroscopy of hemoglobin. *In* Methods in Enzymology. E. Antonini, L. Rossi-Bernardi, and E. Chiancone, editors. Academic Press, New York. 175–261.

Ferrone, F. A., J. Hofrichter, and W. A. Eaton. 1985a. Kinetics of sickle hemoglobin polymerization II: a double nucleation mechanism. *J. Mol. Biol.* 183:611–631.

Ferrone, F. A., J. Hofrichter, and W. A. Eaton. 1985b. Kinetics of sickle hemoglobin polymerization I: studies using temperature-jump and laser photolysis techniques. *J. Mol. Biol.* 183:591–610.

Ferrone, F. A., J. Hofrichter, H. Sunshine, and W. A. Eaton. 1980. Kinetic studies on photolysis-induced gelation of sickle cell hemoglobin suggest a new mechanism. *Biophys. J.* 32:361–377.

Hall, R. S., Y. S. Oh, and C. S. Johnson, Jr. 1980. Photon correlation spectroscopy in strongly absorbing and concentrated samples with applications to unliganded hemoglobin. *J. Phys. Chem.* 84:756–767.

Hofrichter, J. 1986. Kinetics of sickle hemoglobin polymerization III. Nucleation rates determined from stochastic fluctuations in polymerization progress curves. *J. Mol. Biol.* 189:553–571.

Hofrichter, J., P. D. Ross, and W. A. Eaton. 1976. Supersaturation in sickle cell hemoglobin solutions. *Proc. Natl. Acad. Sci. USA.* 73:3035–3039.

Kam, Z., and J. Hofrichter. 1986. Quasi-elastic laser light scattering from solutions and gels of hemoglobin S. *Biophys. J.* 50:1015–1020.

Mickols, W., M. F. Maestre, I. Tinoco, and S. H. Embury. 1985. Visualization of oriented hemoglobin S in individual erythrocytes by differential extinction of polarized light. *Proc. Natl. Acad. Sci. USA.* 82:6527–6531.

Prouty, M. S., A. N. Schechter, and V. A. Parsegian. 1985. Chemical potential measurements of deoxyhemoglobin S polymerization. *J. Mol. Biol.* 184:517–528.

Samuel, R. E., E. D. Salmon, and R. W. Briehl. 1990. Nucleation and growth of fibres and gel formation in sickle cell haemoglobin. *Nature (Lond.).* 345:833–835.

Sunshine, H. R., J. Hofrichter, and W. A. Eaton. 1979. Gelation of sickle cell hemoglobin in mixtures with normal adult and fetal hemoglobins. *J. Mol. Biol.* 133:435–467.

White, J. G., and B. Heagan. 1970. The fine structure of cell free sickled hemoglobin. *Am. J. Pathol.* 58:1–17.

Zhou, H. X., and F. A. Ferrone. 1990. Theoretical description of the spatial dependence of sickle hemoglobin polymerization. *Biophys. J.* 58:695–703.